

Research Article

I-V Characteristics of Pt_xCo_{1-x} ($x = 0.2, 0.5$, and 0.7) Thin Films

M. Erkovan,^{1,2} E. Şentürk,³ Y. Şahin,⁴ and M. Okutan⁵

¹ Department of Physics, Gebze Institute of Technology, 41400 Gebze, Kocaeli, Turkey

² Metallurgical and Materials Engineering, Sakarya University, 54187 Esentepe, Sakarya, Turkey

³ Department of Physics, Sakarya University, 54187 Esentepe, Sakarya, Turkey

⁴ Council of Forensic Medicine, 34196 Istanbul, Turkey

⁵ Department of Physics, Yildiz Technical University, Davutpasa, 34210 Istanbul, Turkey

Correspondence should be addressed to M. Okutan; okutan@yildiz.edu.tr

Received 27 April 2013; Revised 2 July 2013; Accepted 4 July 2013

Academic Editor: Mengnan Qu

Copyright © 2013 M. Erkovan et al. This is an open access article distributed under the Creative Commons Attribution License, which permits unrestricted use, distribution, and reproduction in any medium, provided the original work is properly cited.

Three different chemical ratios of Pt_xCo_{1-x} thin films were grown on p-type native oxide Si (100) by Magneto Sputtering System with cosputtering technique at 350°C temperature to investigate electrical prosperities. X-ray photoelectron spectroscopy analysis technique was used to specify chemical ratios of these films. The current-voltage (*I-V*) measurements of metal-semiconductor (MS) Schottky diodes were carried out at room temperature. From the *I-V* analysis of the samples, ideality factor (*n*), barrier height (ϕ), and contact resistance values were determined by using thermionic emission (TE) theory. Some important parameters such as barrier height, ideality factor, and serial resistance were calculated from the *I-V* characteristics based on thermionic emission mechanism. The ideality factors of the samples were not much greater than unity, and the serial resistances of the samples were also very low.

1. Introduction

Thin films have nowadays very wide usage area in technological applications [1–6]. They show very distinct difference from bulk films such as Curie temperature and the electrical properties. They get more and more important with the preparation systems progress. In particular after Ultra High Vacuum (UHV) systems became popular, they have been prepared with good quality and cleanness [1]. There are several preparation techniques to meet user's need. Some of them for UHV systems are magnetron sputtering deposition, molecular beam epitaxial and e-beam evaporation, and pulse laser deposition [7]. Due to the advantages of the preparation techniques, thin films started being used widely in technological applications such as optics [2], optoelectronics [3], electronics [4], magnetic applications [5], and sensors [6]. Firstly, thin films were prepared as a single layer with monoelement structure. After a little while due to some technological requirements, they started being prepared as multilayer structures and alloy forms with two or more elements. Multilayer forms started to be popular after Giant

Magneto Resistance (GMR) [8, 9] effect and Tunneling Magneto Resistance (TMR) [10] effect were observed in the 1980s. The other thin film form is alloy film which started solving some of technological problems, and they gained more importance when compared to single layer films. When two or more elements compose themselves to be alloys, generally every one of them loses some of its own properties and gains new properties. PtCo alloys are very good examples to clarify this situation due to magnetic properties [11]. Platinum is naturally nonmagnetic material so it has not got any magnetic moment [12]. When it composes its with ferromagnetic cobalt, it gains some net magnetic moment and starts behaving as a magnetic material as a paramagnetic and also changes the magnetic properties of cobalt [13]. For example, the magnetocrystalline anisotropy is a key parameter for data storage media. Pt affects the magnetocrystalline anisotropy of cobalt. The magnetocrystalline anisotropy constant of Cobalt ($410 \text{ KJ}\cdot\text{m}^{-3}$) [14] is ten times smaller than the magnetocrystalline anisotropy constant of PtCo ($4,9 \text{ MJ}\cdot\text{m}^{-3}$) [14]. SmCo₅ are used now for data storage media, and the magnetocrystalline anisotropy

constant PtCo is very close to SmCo_5 's ($17.2 \text{ MJ} \cdot \text{m}^{-3}$) [14], so PtCo alloy still is an active research area and the one of good candidates is for next generation data storage media [15]. Besides their magnetic properties, PtCo alloys also have catalytic properties [16–20]. Another most important point is that they can be prepared easily in different chemical ratios, and their phase is very stable [21]. We believe that if these structures come into use in next generation magnetic data storage media, their electrical properties may be gained significantly.

The other hand semiconductor base materials exhibit an interesting combination of magnetic and electrical properties, which are essential for future generation spintronics device applications [22]. Two of these electrical properties are Schottky barriers (SB) and tunneling diode.

They can be used in microwave detector diodes [23]. Schottky diodes with low barrier height have some applications in devices operating as infrared detectors and imaging sensors at high frequencies [24, 25]. Schottky Metal (SM) contacts have an important role in electronic technology [26, 27]. Metal-semiconductor (MS) contact is one of the most widely used rectifying contacts in electronic industry [28, 29]. Electronic properties of a Schottky diode are characterized by its series resistance, barrier height, and ideality factor parameters [30, 31]. Schottky barrier height, and other characteristic parameters can affect device performance, stability and reliability [32–35]. Electrical properties of PtCo alloys have not been investigated so far. So in this study, we focused on surface and volume resistivity of different stoichiometry of PtCo alloys films. In order to realize this goal, we prepared three different chemical ratios of $\text{Pt}_x\text{Co}_{1-x}$ ($x = 0.2, 0.5, 0.7$) alloy films with magnetron sputtering technique at UHV conditions. X-ray photoelectron spectroscopy was used to determine the chemical ratio of the films and the deposition rate of Pt and Co.

In the scope of this work, the $\text{Pt}_x\text{Co}_{1-x}$ ($x = 0.2, 0.5, 0.7$) alloy films were prepared for the new generation data storage and catalytic material by Magneto Sputtering System. They were examined with current-voltage (I - V) measurement techniques. This method is a reliable tool for investigating the behaviors of electrical properties and for optimizing metal-semiconductor and magnetic-semiconductor materials.

2. Experiments

All the experiments were performed in a cluster Ultra High Vacuum (UHV) chamber. The chamber is combined with magnetron sputtering deposition chamber and analytical chamber. There is a load-lock chamber between them. PtCo alloy films were grown on native p-type Si (100) substrate by magnetron sputtering deposition technique with base pressure $< 1 \times 10^{-8}$ mbar. All the substrates were cleaned with ethanol and methanol baths before being transferred into UHV conditions. Then they were subjected to annealing process at 600°C for 30 minutes by a pyrolytic boron nitride (PBN) heater which is located under the substrate at the sample holder. It has the capability of annealing up to 1200°C . The sample holder is cooled by chilled water to

hold the sample temperature for different processes. For deposition, Ar process gas (6N purity) was exposed to the magnetron sputtering chamber so the base pressure level increased to 1.3×10^{-3} – 1.4×10^{-4} mbar. In order to prepare $\text{Pt}_x\text{Co}_{1-x}$ ($x: 0.2, 0.5, 0.7$) alloy films, the Pt (99.99% purity) and Cobalt (99.98% purity) elemental targets were used. Their sizes are three inches to provide uniform deposition surface. The distance between the substrate and target was 100 mm and always kept for all growth process. Thickness calibration of the films was conducted with Quartz Crystal Monitoring (QCM) during deposition in situ. X-ray photoelectron spectroscopy (XPS) was used for QCM calibration. Before synthesizing PtCo alloy films, both Pt and Co deposition ratios were calculated. $\text{Pt}_x\text{Co}_{1-x}$ ($x: 0.2, 0.5, 0.7$) alloy films were grown using cosputtering technique. The number of sequences was kept 100 for all samples; on the other hand, the Pt and Co deposition time was calculated depending on the chemical ratio of $\text{Pt}_x\text{Co}_{1-x}$ ($x: 0.2, 0.5, 0.7$) alloy films. The power applied to Co target was 30 Watt and the corresponding deposition rate was $0.3 \text{ \AA}/\text{sec}$. The Pt deposition rate was $0.1 \text{ \AA}/\text{sec}$ with 2 Watt. The Pt and Co targets were operated at the same time, and the temperature was held at 350°C . The films thicknesses were 300 \AA .

The current-voltage (I - V) and resistivity of the thin films were studied using a four-point probe measurement with the Lucas Signatone system. I - V and surface resistance were measured using a Keithley 2400 Source-Meter in a four-point probe technique and converted to the surface resistivity. The I - V and surface resistance measurements were carried out at room temperature.

3. Result and Discussion

XPS was used to determine the selected chemical ratios of alloy films in situ. Figure 1 shows survey XPS spectra for $\text{Pt}_{0.5}\text{Co}_{0.5}$ and $\text{Pt}_{0.7}\text{Co}_{0.3}$. High resolution XPS spectra for the major photoemission Co 2p and Pt 4f regions were also taken (Figure 2) for analysis in commercial software CasaXPS 2.3.14. We used the Shirley background function to fit and analyze the peaks. The Voigt function identifying the photoemission nature was used to calculate the peak area of Co and Pt. The calculated peak areas of Co and Pt were divided by the atomic sensitivity factors (ASFs) which depend on both elemental properties and XPS setup (3.59 for Pt 4f, and 5.75 for Co 2p). The calculated Pt to Co ratios within alloy films are 20 : 80, 50 : 50, and 70 : 30.

Beside these analyses, the XPS spectra were given both Pt peaks and Co peaks from both their pure and the $\text{Pt}_{0.6}\text{Co}_{0.4}$ films (Figure 3). Because of their alloy form, both Pt and Co peaks came from $\text{Pt}_{0.6}\text{Co}_{0.4}$ films; they are shifted from the low binding energy value to the high binding energy value. Their peak shape also expanded due to their chemical bonding.

The typical forwarded bias voltage (V) and current (I) characteristics obtained from the samples are shown in Figure 4. I - V curves of the samples are linear at low bias voltage and nonlinear at high bias voltage. All the curves

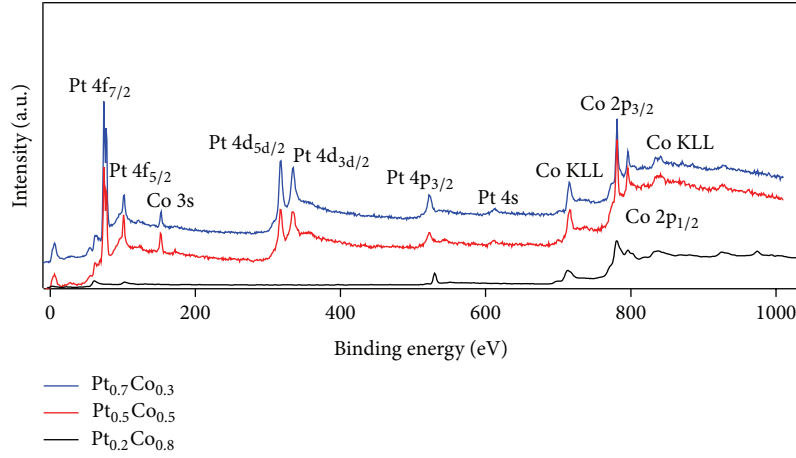


FIGURE 1: XPS survey spectra from the alloy surface of the $\text{Pt}_{0.2}\text{Co}_{0.8}$, $\text{Pt}_{0.5}\text{Co}_{0.5}$, and $\text{Pt}_{0.7}\text{Co}_{0.3}$ films.

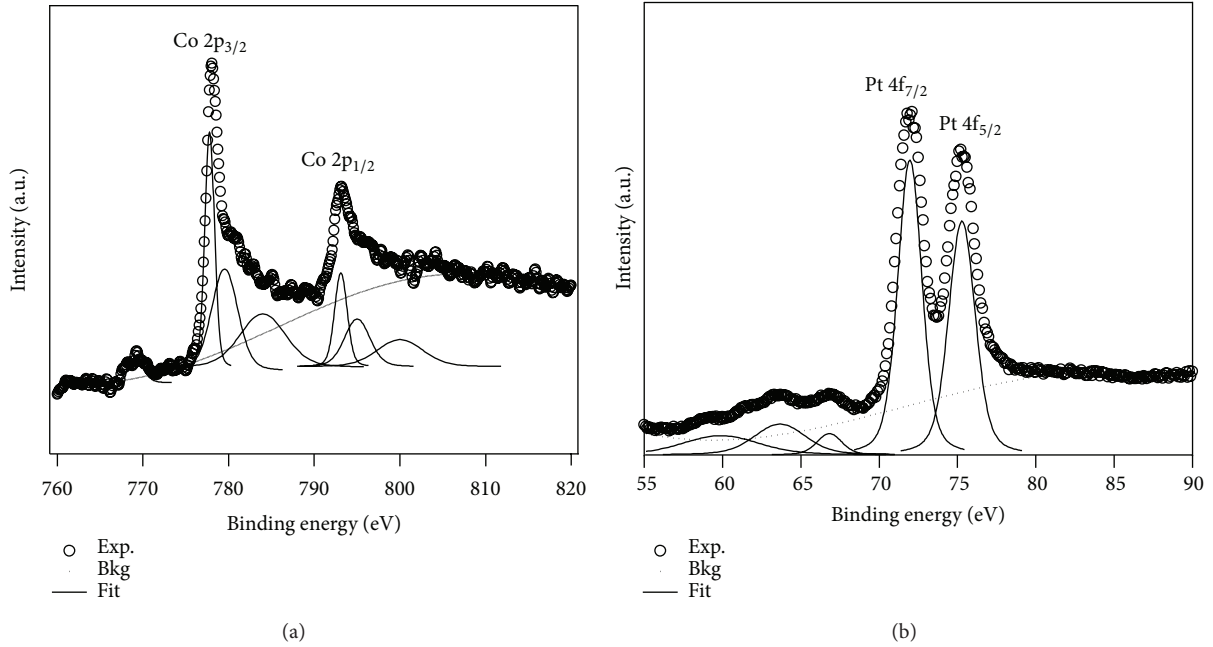


FIGURE 2: XPS spectrum from $\text{Pt}_{0.5}\text{Co}_{0.5}$ for both Pt and Co major peaks. The ratios of peak areas under the Pt 4f and Co 2p regions provide the ratio of Pt and Co atoms.

show an intersection at low forward biases (about 0.1–0.2 V). The I - V curvature quickly (at low forward bias) becomes dominant with a resistance from contact wires or bulk resistance of the samples. If the current passes through MS Schottky diode at a forward bias voltage ($3kT/q \leq V$), a high resistive potential barrier created by grains is considered in these systems [36]. The observed results require a serial resistance [37]. Serial or parasitic resistance, R_s , includes bulk and contact resistances. The I - V results deviated from ideality can be explained by thermionic emission theory with a serial resistance. The TE model considers that I - V characteristic of an MS type Schottky diode is given as follows [38]:

$$I = I_o \exp\left(\frac{q(V - IR_s)}{nkT}\right) \left[1 - \exp\left(-\frac{q(V - IR_s)}{kT}\right)\right], \quad (1)$$

where q is electron charge, k is Boltzmann constant, T is absolute temperature, n is ideality factor (close to 1), and finally I_o is saturation current. $V - IR_s$ is voltage drop across the diode. The saturation current can be written as

$$I_o = AA^* T^2 \exp\left(-\frac{q\phi_b}{kT}\right), \quad (2)$$

where ϕ_b , A , and A^* are apparent barrier height, effective contact area, and Richardson constant, respectively. All these physical parameters have an importance for technological application. Richardson constant is equal to $32 \text{ Acm}^{-2} \text{ K}^{-2}$ for p-type Si [39]. The saturation current can be obtained from an extrapolation to current axis in I - V plot at zero bias voltage. At relatively high forward bias voltages, the parasitic or serial resistance goes to a constant value. In general, low serial resistance is required for a device application [40, 41].

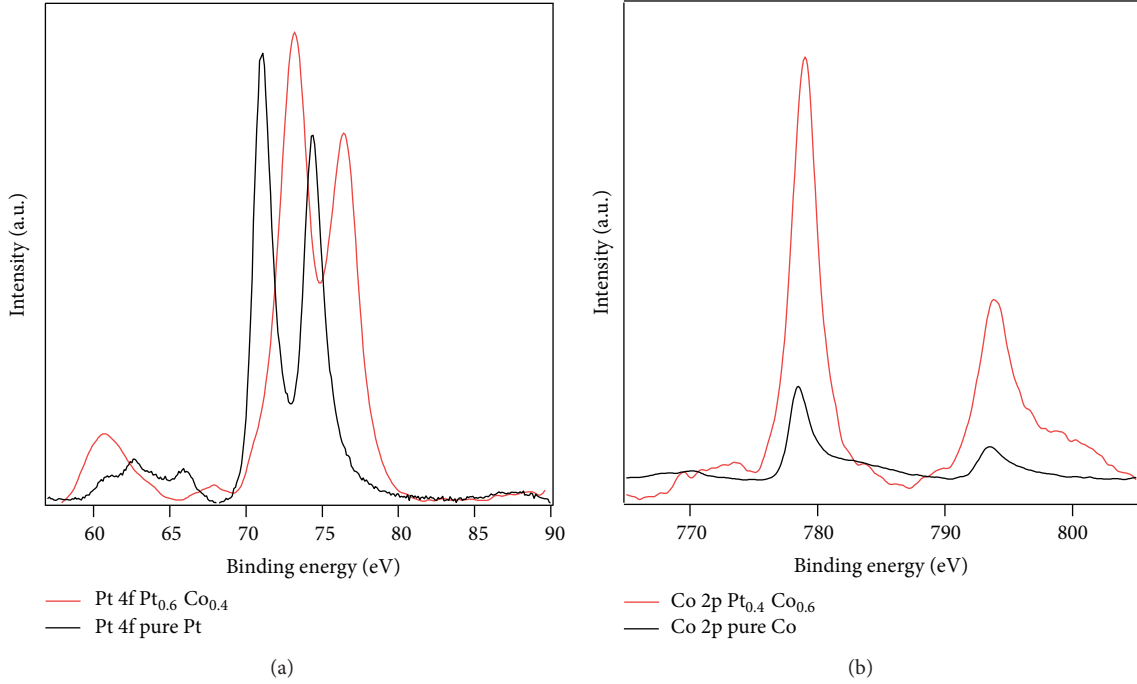


FIGURE 3: The comparison of both Pt 4f and Co 2p peaks that came from both their pure films and Pt_{0.6}Co_{0.4} films.

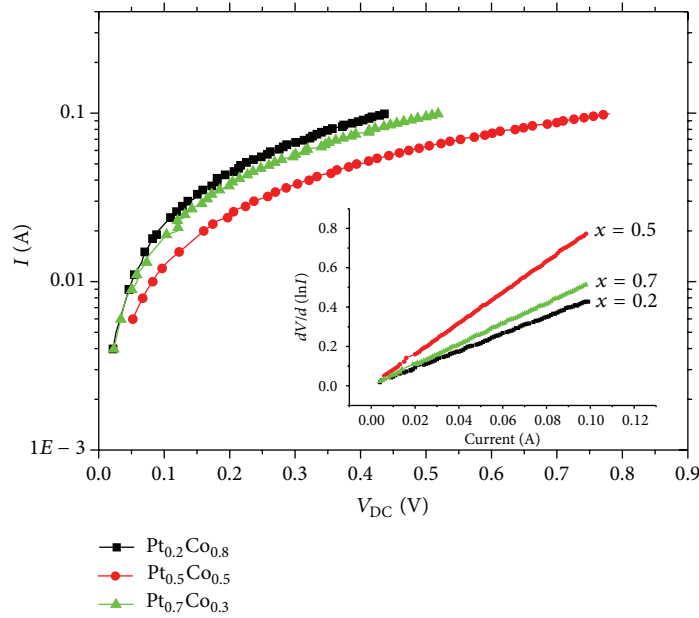


FIGURE 4: Current-voltage graph and inset: $dV/d(\ln I) - I$ plot.

The series resistance, ideality factor, and barrier height are determined by using Cheung's functions as follows [42]:

$$\frac{dV}{d(\ln I)} = IR_s + \frac{nkT}{q}, \quad (3)$$

$$H(I) = V(I) - \frac{nkT}{q} \ln\left(\frac{I}{AA^*T^2}\right), \quad (4)$$

and another form of $H(I)$ function is given as follows:

$$H(I) = n\phi_b + IR_s. \quad (5)$$

The $dV/d(\ln I) - I$ plot is shown in inset of Figure 4. All curves are straight lines with low and different slopes. The ideality factor can be obtained by using (3) from the slope of the linear curves. The obtained values of the ideality factor are given in Table 1. It is clear from the table that the values

TABLE 1: I - V characteristics parameters of the samples.

	R_s (Ω)	n	ϕ_b (eV)
$x = 0.2$	3.89	1.32	0.26
$x = 0.5$	6.64	1.83	0.27
$x = 0.7$	4.60	1.03	0.25

of the ideality factor for the samples are really low. The low values (~ 1) of the ideality factor may result from homogeneity of film thickness [43], series resistance effect, low interface state, and the interface charges.

The simple analysis of (5) yields n and ϕ_b parameters. The change in R_s , n , and ϕ_b with composition at room temperature is shown in Table 1. It is clear from the data obtained from Figure 4 that the parameters have strong composition dependence.

4. Conclusion

This work indicates that coating of p-type Si (100) with $\text{Pt}_x\text{Co}_{1-x}$ alloys thin films can be prepared by Magnetron Sputtering Deposition at UHV condition. XPS was used for three different goals. One was to determine the deposition rate of cobalt and platinum. The other one was determination of the chemical ratio of PtCo alloy films. The last one was that the PtCo alloy forms were proved by XPS results. The performance and reliability of metal-semiconductor or metal-insulator-semiconductor diodes depend on barrier height, properties of interface layer, and R_s . I - V characteristics of the samples were investigated at room temperature. The nonideal type I - V behavior observed was attributed to a serial resistance in the MS type Schottky diode. The serial resistances were found to be 3.89 Ω , 6.64 Ω and 4.60 Ω for $x = 0.2$, 0.5, and 0.7, respectively.

Acknowledgments

This work was partially supported by TÜBİTAK (The Scientific and Technological Research Council of Turkey) through the project no. 212T217 and Yildiz Technical University through the project no. 2011-01-01-KAP01. The authors gratefully acknowledge that all samples used in this study were grown at the Nanotechnology Center of Gebze Institute of Technology.

References

- [1] R. F. Soohoo, *Magnetic Thin Films*, Harper and Row, New York, NY, USA, 1965.
- [2] D. E. Aspnes, "Optical properties of thin films," *Thin Solid Films*, vol. 89, no. 3, pp. 249–262, 1982.
- [3] G. Eda and M. Chhowala, "Chemically derived graphene oxide: towards large-area thin-film electronics and optoelectronics," *Advanced Materials*, vol. 22, no. 22, pp. 2392–2415, 2010.
- [4] M. S. Boon, W. P. S. Saw, and M. Mariatti, "Magnetic, dielectric and thermal stability of NiZn ferrite-epoxy composite thin films for electronic applications," *Journal of Magnetism and Magnetic Materials*, vol. 324, no. 5, pp. 755–760, 2012.
- [5] M. Erkovan, R. Topkaya, S. T. Öztürk, M. Özdemir, B. Aktaş, and O. Öztürk, "Ferromagnetic resonance investigation of Py/Cr multilayer system," *Journal of Applied Physics*, vol. 110, no. 2, Article ID 023908, 6 pages, 2011.
- [6] G. Sberveglieri, "Recent developments in semiconducting thin-film gas sensors," *Sensors and Actuators B*, vol. 23, no. 2-3, pp. 103–109, 1995.
- [7] T. Shima and K. Takanashi, "Hard magnetic thin films," in *Handbook of Magnetism and Advanced Magnetic Materials*, vol. 4, Wiley & Sons, Chichester, UK, 2007.
- [8] M. N. Baibich, J. M. Broto, A. Fert et al., "Giant magnetoresistance of (001)Fe/(001)Cr magnetic superlattices," *Physical Review Letters*, vol. 61, no. 21, pp. 2472–2475, 1988.
- [9] G. Binasch, P. Grünberg, F. Saurenbach, and W. Zinn, "Giant magnetoresistance in antiferromagnetic Co/Cu multilayers," *Physical Review B*, vol. 39, p. 7, 1991.
- [10] J. S. Moodera, L. R. Kinder, T. M. Wong, and R. Meservey, "Large magnetoresistance at room temperature in ferromagnetic thin film tunnel junctions," *Physical Review Letters*, vol. 74, no. 16, pp. 3273–3276, 1995.
- [11] M. Öztürk, E. Sınır, E. Demirci, M. Erkovan, O. Öztürk, and N. Akdoğan, "Exchange bias properties of $[\text{Co}/\text{CoO}]_n$ multilayers," *Journal of Applied Physics*, vol. 112, Article ID 093911, 2012.
- [12] E. E. Shalyguina and K. Shin, "Influence of nonmagnetic layer (Ti, Zr, Pt) on magnetic and magneto-optical properties of Fe/NML bilayers and Fe/NML/Fe trilayers," *Journal of Magnetism and Magnetic Materials*, vol. 220, no. 2-3, pp. 167–174, 2000.
- [13] J. Wang, T. Sannomiya, J. Shi, and Y. Nakamura, "Influence of interface roughness on the exchange bias of Co/CoO multilayers," *Journal of Applied Physics*, vol. 113, no. 17, Article ID 17D707, 3 pages, 2013.
- [14] J. M. D. Coey, *Magnetism and Magnetic Materials*, Cambridge University, Cambridge, UK, 2010.
- [15] N. Sharma, G. A. Jones, S. M. Casey, and P. J. Grundy, "The microstructure and magnetic properties of cobalt-rich Co-Pt alloy thin films grown using ion-beam-assisted deposition," *Journal of Physics D*, vol. 31, no. 21, pp. 3020–3027, 1998.
- [16] V. R. Stamenkovic, B. S. Mun, M. Arenz et al., "Trends in electrocatalysis on extended and nanoscale Pt-bimetallic alloy surfaces," *Nature Materials*, vol. 6, no. 3, pp. 241–247, 2007.
- [17] U. Bardi, A. Atrei, E. Zanazzi, G. Rovida, and P. N. Ross, "Study of the reconstructed (001) surface of the $\text{Pt}_{80}\text{Co}_{20}$ alloy," *Vacuum*, vol. 41, no. 1-3, pp. 437–440, 1990.
- [18] U. Bardi, B. C. Beard, and P. N. Ross, "CO chemisorption on the [111] and [100] oriented single crystal surfaces of the alloy CoPt_3 ," *Journal of Catalysis*, vol. 124, no. 1, pp. 22–29, 1990.
- [19] Y. Kiros, "Electrocatalytic properties of Co, Pt, and Pt-Co on carbon for the reduction of oxygen in alkaline fuel cells," *Journal of the Electrochemical Society*, vol. 143, no. 7, pp. 2152–2157, 1996.
- [20] L. Xiong, A. M. Kannan, and A. Manthiram, "Pt-M (M1/4Fe, Co, Ni and Cu) electrocatalysts synthesized by an aqueous route for proton exchange membrane fuel cells," *Electrochemistry Communications*, vol. 4, no. 11, pp. 898–903, 2002.
- [21] J. H. Cho, B. Y. Kim, H. D. Kim et al., "Enhanced ferromagnetism in Co-doped TiO_2 powders," *Physica Status Solidi B*, vol. 241, no. 7, pp. 1537–1540, 2004.
- [22] N. W. Ashcroft and N. D. Mermin, *Solid State Physics*, Saunders College, London, UK, 1976.
- [23] J. N. Schulman, V. Kolinko, M. Morgan et al., "W-band direct detection circuit performance with Sb-heterostructure diodes,"

- IEEE Microwave and Wireless Components Letters*, vol. 14, no. 7, pp. 316–318, 2004.
- [24] M. Kimata, “Metal silicide Schottky infrared detector arrays,” in *Infrared Detectors and Emitters: Materials and Devices*, P. Capper and C. T. Elliott, Eds., pp. 77–98, Kluwer Academic, Boston, Mass, USA, 2000.
- [25] W. F. Kosonocky, “State of the art in Schottky-barrier IR image sensors,” in *Infrared Detectors and Focal Plane Arrays II*, Proceedings of SPIE, pp. 2–19, April 1992.
- [26] X. Lu, X. Xu, N. Wang, Q. Zhang, and M. C. Lin, “Chemisorption and decomposition of thiophene and furan on the Si(100)- 2×1 surface: a quantum chemical study,” *Journal of Physical Chemistry B*, vol. 105, no. 41, pp. 10069–10075, 2001.
- [27] M. Biber, M. Çakar, and A. Türüt, “The effect of anodic oxide treatment on n-GaAs Schottky barrier diodes,” *Journal of Materials Science*, vol. 12, no. 10, pp. 575–579, 2001.
- [28] G. Liang, T. Cui, and K. Varahramyan, “Electrical characteristics of diodes fabricated with organic semiconductors,” *Microelectronic Engineering*, vol. 65, no. 3, pp. 279–284, 2003.
- [29] G. Liang, T. Cui, and K. Varahramyan, “Fabrication and electrical characteristics of polymer-based Schottky diode,” *Solid-State Electronics*, vol. 47, no. 4, pp. 691–694, 2003.
- [30] M. Okutan, E. Basaran, and F. Yakuphanoglu, “Electronic and interface state density distribution properties of Ag/p-Si Schottky diode,” *Applied Surface Science*, vol. 252, no. 5, pp. 1966–1973, 2005.
- [31] M. Okutan and F. Yakuphanoglu, “Analysis of interface states and series resistance of Ag/SiO₂/n-Si MIS Schottky diode using current-voltage and impedance spectroscopy methods,” *Microelectronic Engineering*, vol. 85, no. 3, pp. 646–653, 2008.
- [32] P. L. Hanselaer, W. H. Laflère, R. L. van Meirhaeghe, and F. Cardon, “Current-voltage characteristic of Ti-pSi metal-oxide-semiconductor diodes,” *Journal of Applied Physics*, vol. 56, no. 8, pp. 2309–2314, 1984.
- [33] G. Liang, T. Cui, and K. Varahramyan, “Fabrication and electrical characteristics of polymer-based Schottky diode,” *Solid-State Electronics*, vol. 47, no. 4, pp. 691–694, 2003.
- [34] S. M. Sze, *Physics of Semiconductor Devices*, Wiley, New York, NY, USA, 2nd edition, 1981.
- [35] E. H. Rhoderick, *Metal-Semiconductor Contacts*, vol. 121 of p. 136, Oxford University Press, Oxford, UK, 1978.
- [36] R. Gross, L. Alff, B. Büchner et al., “Physics of grain boundaries in the colossal magnetoresistance manganites,” *Journal of Magnetism and Magnetic Materials*, vol. 211, no. 1–3, pp. 150–159, 2000.
- [37] B. Kinaci, S. Şebnem Çetin, A. Bengi, and S. Özçelik, “The temperature dependent analysis of Au/TiO₂ (rutile)/n-Si (MIS) SBDs using current-voltage-temperature (*I-V-T*) characteristics,” *Materials Science in Semiconductor Processing*, vol. 15, no. 5, pp. 531–535, 2012.
- [38] H. Uslu, Ş. Altındal, U. Aydemir, I. Dökme, and I. M. Afandiyeva, “The interface states and series resistance effects on the forward and reverse bias *I-V*, *C-V* and *G/ω-V* characteristics of Al-TiW-Pd 2Si/n-Si Schottky barrier diodes,” *Journal of Alloys and Compounds*, vol. 503, no. 1, pp. 96–102, 2010.
- [39] A. Tataroğlu and S. Altındal, “Analysis of interface states and series resistance of MIS Schottky diodes using the current-voltage (*I-V*) characteristics,” *Microelectronic Engineering*, vol. 85, no. 1, pp. 233–237, 2008.
- [40] N. Tuğluoğlu and S. Karadeniz, “Analysis of current-voltage and capacitance-voltage characteristics of perylene-monoimide/n-Si Schottky contac,” *Current Applied Physics*, vol. 12, no. 6, pp. 1529–1535, 2012.
- [41] S. Demirezen, Z. Sönmez, U. Aydemir, and S. Altındal, “Effect of series resistance and interface states on the *I-V*, *C-V* and *G/ω-V* characteristics in Au/Bi-doped polyvinyl alcohol (PVA)/n-Si Schottky barrier diodes at room temperature,” *Current Applied Physics*, vol. 12, no. 1, pp. 266–272, 2012.
- [42] R. Şahingöz, H. Kanbur, M. Voigt, and C. Soykan, “The determination of interface states and series resistance profile of Al/polymer/PEDOT-PSS/ITO heterojunction diode by *I-V* and *C-V* methods,” *Synthetic Metals*, vol. 158, no. 17–18, pp. 727–731, 2008.
- [43] M. B. Reddy, A. A. Kumar, V. Janardhanam, V. R. Reddy, and P. N. Reddy, “Rapid thermal annealing effects on electrical and structural properties of Pd/Au Schottky contacts to n-type InP(111),” *Current Applied Physics*, vol. 9, pp. 972–977, 2009.

